Regulation of the Collisional Self-Quenching of Fluorescence in Clay/Porphyrin Complex by Strong Host-Guest Interaction

ARTICLE *in* THE JOURNAL OF PHYSICAL CHEMISTRY A · NOVEMBER 2012

Impact Factor: 2.69 · DOI: 10.1021/jp309502j · Source: PubMed

5 AUTHORS, INCLUDING:

Shinsuke Takagi
Tokyo Metropolitan University
86 PUBLICATIONS **1,489** CITATIONS

THE JOURNAL OF PHYSICAL CHEMISTRY A

Article

pubs.acs.org/JPCA

Regulation of the Collisional Self-Quenching of Fluorescence in Clay/Porphyrin Complex by Strong Host−Guest Interaction

Yohei Ishida,[†,‡] Tetsuya Shimada,[†] Hiroshi Tachibana,[†] Haruo Inoue,[†] and Shinsuke Takagi*[,†,§]

[†]Department of Applied Chemistry, Graduate Course of Urban Environmental Sciences, Tokyo Metropolitan University, Minami-ohsawa 1-1, Hachiohji, Tokyo 192-0397, Japan

[‡]Japan Society for the Promotion of Science (DC1), Ichibancho, Chiyoda-ku, Tokyo 102-8471, Japan

[§]PRESTO (Precursory Research for Embryonic Science and Technology), Japan Science and Technology Agency, 4-1-8 Honcho Kawaguchi, Saitama, Japan

Supporting Information

ABSTRACT: This paper proposes a novel methodology to improve noncollisional photochemical reactions such as Förster resonance energy transfer on solid surfaces. Since an excited guest molecule densely adsorbed on the solid surfaces is quenched by an unfavorable interaction between guests in general, the photochemical reactions such as electron and energy transfers tend to be inefficient compared to those in homogeneous systems. In this work, the mechanism of unfavorable quenching process of dyes on the clay surface as a typical solid surface for the photochemical energy transfer was systematically investigated by using a series of porphyrin derivatives. As a result, it was found that the quenching rate constants of excited guest dye determined by the time-resolved fluorescence measurements correlated well with the strengths of coulombic interaction between host and guest. The strong coulombic interaction should suppress the mobility and collision frequency of guests on the clay surface; thus, the collision of guest molecules was revealed as the origin of unfavorable quenching for photochemical reactions on the clay surface. According to this principle, we will be able to construct efficient photochemical reaction systems without any quenching process, such as efficient energy transfers toward an artificial light-harvesting system. In fact, we have already realized almost 100% energy transfer by the suppression of quenching process on the clay surface (e.g., *J. Am. Chem. Soc.* **2011**, *133*, 14280−14286).

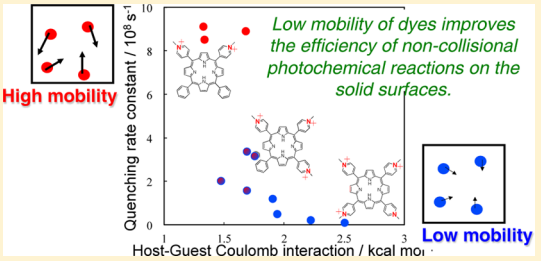

INTRODUCTION

Photochemical reactions such as electron and energy transfers highly depend on the distance between reactants. Generally a short intermolecular distance, which leads to a large reaction rate constant, is preferred for photochemical reactions; thus, recently the high-density adsorption structure of functional dyes on solid surfaces has been studied extensively for constructing efficient photochemical reaction systems.[1−19] However, because an excited guest molecule densely adsorbed on the solid surfaces is usually quenched by an unfavorable interaction between guests, photochemical reaction tends to be inefficient compared to those in homogeneous systems. This unfavorable quenching process of the excited state is generally called "self-quenching". Many researchers have been investigating the self-quenching for constructing efficient photochemical reaction systems.[20−31] However, since a self-quenching includes various types of possible mechanisms and we cannot distinguish them definitely, the mechanism of self-quenching has not been revealed entirely.

A self-quenching is a quenching process of excited state molecule due to an interaction between the same types of molecules. The mechanism of the interaction is classified into a static process and a dynamic process.[20−31] Under the static process,[20−23] an aggregation of molecules is the main factor to induce a self-quenching. Generally an aggregation is defined as an interaction between transition dipole moments of dyes. Thus, the aggregation is easily detected as absorption spectral changes. Because it is difficult to suppress an aggregation of molecules in usual systems on solid surfaces, the investigations for the self-quenching tend to be complicated and the dilution of the adsorption density of dyes has been the major methodology to suppress the aggregation. In contrast, we have reported an interesting clay/porphyrin complex in which the porphyrin molecules adsorb on the clay surface without aggregation even under high dye loadings.[7−16] Since the aggregation of dyes is completely suppressed in our clay/porphyrin system, static self-quenching is negligible. Thus, the mechanism for the self-quenching can be simply discussed only as the dynamic processes in our clay/dye system.

Dynamic self-quenching processes can be mainly classified into two kinds of origin,[24−31] i.e., (i) an electron transfer reaction and/or an enhanced thermal deactivation process due to the collision of molecules and (ii) a chemical conversion to other compounds. In our system, (ii) is not detected judging

Received: September 25, 2012
Revised: October 31, 2012
Published: November 8, 2012

dx.doi.org/10.1021/jp309502j | J. Phys. Chem. A 2012, 116, 12065−12072

from the fact that the absorption spectra are completely the same shape during the irradiation of the excitation light. Thus, only (i) is the possible origin of self-quenching in the present system.

In this work, the unfavorable self-quenching process of excited guest molecule on the clay surface due to mechanism (i) was systematically investigated by using 11 types of porphyrin derivatives. Since mechanism (i) should depend on the collision frequency of dyes on the clay surface, we examined the steady-state and time-resolved fluorescence measurements under the various adsorption density conditions. Moreover, the governing factor for the self-quenching efficiency due to mechanism (i) was discussed.

The details of our clay/porphyrin systems are as follows. Clay minerals[32−42] are an attractive group of materials that are characterized by (1) nanostructured flat sheets, (2) negatively charged surfaces, (3) exfoliation or stack ability of individual nanosheets depending on the surrounding conditions, and (4) optical transparency in the visible region in the exfoliated state when the particle size is small (c.a. <200 nm). The formation of unique nonaggregated porphyrin assembly on the clay surface was rationalized by a size-matching of distances between the charged sites in the porphyrin molecule and those between anionic sites on the clay surface. We termed this effect a "size-matching rule".[12−15]

EXPERIMENTAL SECTION

Materials. The saponite clay used in this experiment was synthesized by hydrothermal synthesis according to a previous paper.[15] Na_2SiO_3 (15.45 g) solution was diluted by the addition of 80 mL of deionized water, and then 5 mL of nitric acid solution was added to the diluted Na_2SiO_3 solution (solution A). $MgCl_2{\cdot}6H_2O$ (12.44 g) and $AlCl_3{\cdot}6H_2O$ (1.97 g) were dissolved in 20 mL of deionized water (solution B). Solutions A and B were combined, and the obtained solution was added to 52 mL of ammonia solution under continuous stirring within approximately 3 min. The formed precipitate was filtered with a glass filter (type 25G3) and washed with deionized water repeatedly. A 5 mL aqueous solution of NaOH (1.55 M) was added to the collected residue. The obtained slurry was kept under 573 K and 8.5 MPa in an autoclave for about 6 h. The saponite component was collected from the reaction mixture by 3 days hydraulic elutriation and a centrifugal separation of the supernatant (18 000 rpm, 5 h). The synthetic saponite was analyzed with XRD, XRF, ^{27}Al-NMR, FT-IR, and TG/DTA. The cation-exchange capacity (CEC) was 1.00 mequiv g^{-1}, and the average intercharge distance on the clay surface was calculated to be 1.2 nm on the basis of a hexagonal array.

Tetrakis(1-methylpyridinium-4-yl) porphyrin (*p*-4+), tetrakis(1-methylpyridinium-3-yl) porphyrin (*m*-4+), tetrakis-(1-methylpyridinium-2-yl) porphyrin (*o*-4+), zinc tetrakis(1-methylpyridinium-4-yl) porphyrin (Zn*p*-4+), tetrakis(*N,N,N*-trimethylanilinium-4-yl) porphyrin (*A*-4+), zinc tetrakis-(*N,N,N*-trimethylanilinium-4-yl) porphyrin (Zn*A*-4+), tris(1-methylpyridinium-4-yl) monophyenylporphyrin (*p*-3+), tris(1-methylpyridinium-3-yl) monophyenylporphyrin (*m*-3+), tris(1-methylpyridinium-2-yl) monophyenylporphyrin (*o*-3+), *cis*-bis(1-methylpyridinium-4-yl) diphenylporphyrin (*cis-p*-2+), and *trans*-bis(1-methylpyridinium-4-yl) diphenylporphyrin (*trans-p*-2+) were purchased from Frontier Scientific (Figure 1). The counterions were exchanged with chloride ion by use of an ion exchange column (Organo Amberlite IRA400JCL). The purity of porphyrins was checked by ^{1}H NMR. Water was deionized with an ORGANO BB-5A system (PF filter ×2 + G-10 column).

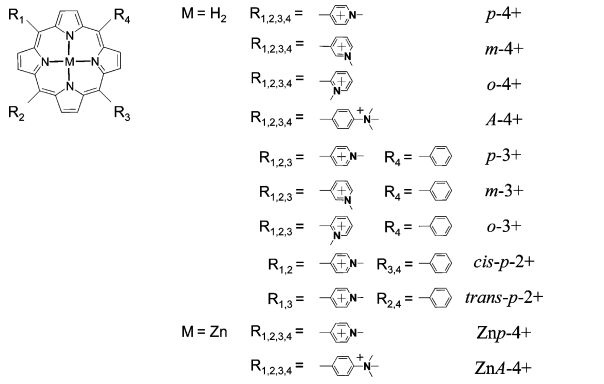

Figure 1. Structures of porphyrins.

Analysis. Absorption spectra were measured with a Shimadzu UV-3150 spectrophotometer. The fluorescence spectra were measured with a Jasco FP-6500 spectrofluorometer. In absorption and fluorescence measurements, a quartz cell was used for the aqueous clay/porphyrin solutions. TG/DTA measurement was carried out with a Shimadzu DTG-60H to determine the water contents of porphyrins and clay. The fluorescence lifetime was measured by a Hamamatsu Photonics C4780 ps fluorescence lifetime measurement system. The excitation light source of the C4780 was a laser diode (406 nm, 71 ps fwhm, 1 kHz). The laser flux was reduced with neutral density filters to avoid nonlinear effects.

Sample Preparation. Measurement for the Steady-State and Time-Resolved Fluorescence Spectra. A typical procedure to prepare clay/porphyrin complexes was as follows. Aqueous solution of porphyrin was mixed with aqueous clay dispersion (9.9 mg L^{-1}) under vigorous stirring. The concentration of porphyrins was 1.0×10^{-7} M. The porphyrin loading level vs cation exchange capacity (CEC) of the clay was adjusted from 0.05 to 70% by changing the volume of the clay dispersion. To express the dye loadings on the clay surface (% vs CEC of the clay), [the number of porphyrin molecules] × 4 was adopted, although the cationic sites in porphyrin molecules are different. This expression excludes the confusion for understanding the adsorption density (molecules/nm^2) for each porphyrin. Actually, tricationic and dicationic dyes act like the tetracationic porphyrins on the clay surface. Under these conditions, the clay sheets exist in a form of individually exfoliated sheets, and the obtained solution was substantially transparent. Since no porphyrin was detected in supernatant liquid obtained by a centrifugation of clay/porphyrin mixture (12 000 rpm, 60 min), all porphyrin molecules adsorb on the clay surface.

Estimation of the Relative Adsorption Equilibrium Constant. An aqueous solution of *p*-4+ was mixed with aqueous clay dispersion under vigorous stirring ([clay] = 2.0 mg L^{-1}, [*p*-4+] = 100% vs CEC). The obtained solution was then mixed with an aqueous solution of another porphyrin (100% vs CEC). The absorption spectrum reached equilibrium after a few minutes. Because the two types of coadsorbed porphyrins exhibited no aggregation on the clay surface, the adsorbed amount of each porphyrin on the clay surface can be determined by the observed absorption spectrum. The relative adsorption equilibrium constants of porphyrin molecules were calculated by the adsorbed and nonadsorbed amounts

dx.doi.org/10.1021/jp309502j | J. Phys. Chem. A 2012, 116, 12065−12072

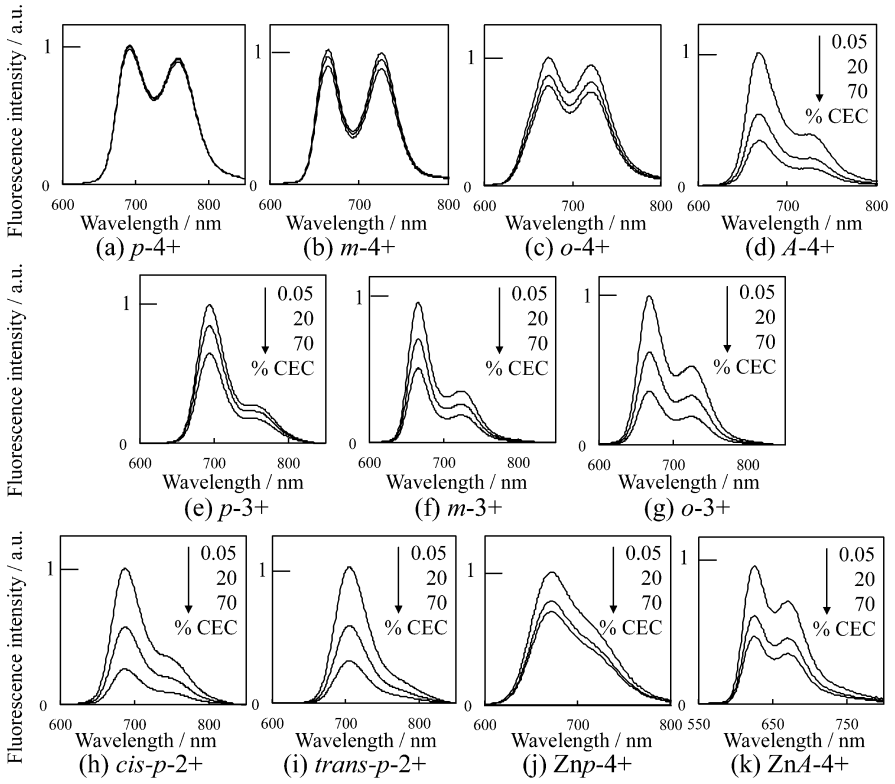

Figure 2. Fluorescence spectra of porphyrin molecules on the clay surface at 0.05%, 20%, and 70% dye loadings of porphyrin vs CEC of the clay: (a) *p*-4+, (b) *m*-4+, (c) *o*-4+, (d) *A*-4+, (e) *p*-3+, (f) *m*-3+, (g) *o*-3+, (h) *cis-p*-2+, (i) *trans-p*-2+, (j) Zn*p*-4+, and (k) Zn*A*-4+. [porphyrin] = 1.0×10^{-7} M. The excitation wavelengths were 406 nm.

determined by the absorption spectra, according to eq 9 as described in the Results and Discussion section.

RESULTS AND DISCUSSION

Steady-State Fluorescence Measurement for Clay/Porphyrin Complexes. Self-quenching behavior of 11 types of cationic porphyrins on an anionic clay surface was investigated by measuring the steady-state fluorescence spectra. Under the present experimental condition, the concentration of porphyrin dyes is always kept constant at 1.0×10^{-7} M, and the dye loading is varied by controlling the concentration of clay, indicating that every sample adsorbed the same number of photons under the same absorbance. We can thus discuss the self-quenching by simply comparing the fluorescence intensity.

The maximum adsorption amount is important because the self-quenching for all porphyrins should be discussed under the same adsorption density condition under the same CEC value. The maximum adsorption amount for *o*-3+ is 70% vs CEC of the clay,[14] which is the minimum value in all of the examined porphyrins. Thus, the self-quenching for all porphyrins will be discussed under 70% CEC conditions, which corresponded to the 2.87 nm intermolecular distance (the calculation is described later). The observed fluorescence spectra of 11 types of porphyrins at 0.05%, 20%, and 70% dye loadings vs CEC of the clay are shown in Figure 2. The self-quenchings of (a) *p*-4+ and (b) *m*-4+ were almost negligible as reported before.[11,16] In the cases of (c) *o*-4+, (e) *p*-3+, and (j) Zn*p*-4+, moderate self-quenchings were observed. A certain amount of self-quenchings was observed for others. In all samples, spectral shapes are completely the same. Because the fluorescence intensity at 0.1% CEC samples was completely the same as those at 0.05% CEC samples for all porphyrins, the fluorescence intensity of 0.05% CEC samples can be used as the standard intensity under the absence of self-quenching. The average intermolecular distance under 0.05% CEC condition is theoretically calculated to be 107 nm, indicating that the self-quenching due to the collision between reactants should be negligible under the condition. The percentage of the self-quenching ratio at 70% CEC ($= 1 - I_{70\%}/I_{0.05\%}$) samples is summarized in Table 1.

Table 1. Percentage of Self-Quenching Ratio at 70% CEC Samples ($= 1 - I_{70\%}/I_{0.05\%}$)

	self-quenching ratio/%
p-4+	2
m-4+	12
o-4+	22
A-4+	66
p-3+	35
m-3+	47
o-3+	64
cis-p-2+	81
trans-p-2+	71
Zn*p*-4+	30
Zn*A*-4+	51

It should be noted that the self-quenchings of these porphyrins are still less than that of typical dyes (such as almost 99% self-quenching of Rhodamine B[20]) due to the size-matching rule.

Time-Resolved Fluorescence Measurements for Clay/Porphyrin Complexes. For the quantitative discussions, the time-resolved fluorescence spectra of porphyrin molecules on

dx.doi.org/10.1021/jp309502j | J. Phys. Chem. A 2012, 116, 12065−12072

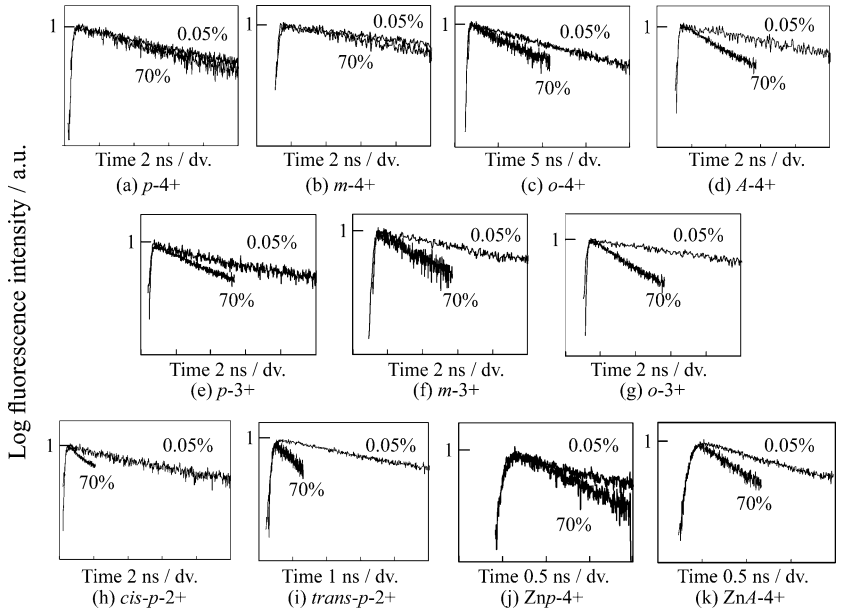

Figure 3. Fluorescence decay profiles for clay/porphyrin complexes at 0.05% and 70% vs CEC: (a) *p*-4+, (b) *m*-4+, (c) *o*-4+, (d) *A*-4+, (e) *p*-3+, (f) *m*-3+, (g) *o*-3+, (h) *cis*-*p*-2+, (i) *trans*-*p*-2+, (j) Znp-4+, and (k) ZnA-4+. [porphyrin] = 1.0×10^{-7} M. The excitation wavelengths were 406 nm.

the clay surface were measured to determine the self-quenching rate constants. The 0.05% CEC samples were measured to determine the excited lifetimes of porphyrin on the clay surface because the self-quenching is negligible under the condition. The 70% CEC samples were observed to determine the self-quenching rate constants.

The typical time-resolved fluorescence spectra are shown in Figure S1. The fluorescence spectral shapes of all samples were completely the same during the decay, as previously reported in the previous paper.[11] The fluorescence decay curves for clay/porphyrin complexes at 0.05% and 70% dye loadings are shown in Figure 3. Because the self-quenching decreases the excited lifetimes, the shorter lifetimes were observed for several porphyrins. As shown in Figure 3, all profiles can be analyzed as single exponential decays. This indicates that all porphyrin molecules have almost the same surrounding conditions and the distribution of adsorbed porphyrins is rather uniform. While the lifetime behavior of dyes on the solid surfaces tends to be complicated due to the aggregation formation, the simple decays were observed in the present system by the effect of the size-matching rule.

The lifetimes at 0.05% CEC (τ_0) and 70% CEC (τ_1) are expressed as eqs 1 and 2:

$$\tau_0 = (k_d + k_f)^{-1} \quad (1)$$

$$\tau_1 = (k_d + k_f + k_{SQ})^{-1} \quad (2)$$

According to eqs 1 and 2, the self-quenching rate constant k_{SQ} is expressed as eq 3

$$k_{SQ} = \frac{1}{\tau_1} - \frac{1}{\tau_0} \quad (3)$$

where k_d is the sum of nonradiative deactivation rate constant and intersystem crossing rate constant of porphyrin molecule, k_f is the radiative deactivation rate constant of molecule, and k_{SQ} is the self-quenching rate constant.

The obtained τ_0, τ_1, and the self-quenching rate constants k_{SQ} are summarized in Table 2.

Table 2. Excited Lifetimes of Porphyrin Molecules on the Clay Surface at 0.05% Dye Loadings (τ_0) and at 70% Dye Loadings (τ_1) and the Calculated Self-Quenching Rate Constants (k_{SQ})

	τ_0/ns	τ_1/ns	$k_{SQ}/10^8$ s^{-1}
p-4+	5.6	5.4	0.1
m-4+	8.9	7.5	0.2
o-4+	9.2	6.2	0.5
A-4+	7.6	2.1	3.5
p-3+	6.2	3.6	1.2
m-3+	7.1	3.3	1.6
o-3+	8.0	3.1	2.0
cis-*p*-2+	6.7	1.0	8.5
trans-*p*-2+	2.9	0.8	9.1
Znp-4+	0.9	0.7	3.2
ZnA-4+	0.9	0.5	8.9

Like this, the self-quenching behaviors of porphyrin molecules on the clay surface were quantitatively analyzed. In the case of *p*-4+, the obtained k_{SQ} is almost zero, indicating that the self-quenching is almost negligible. On the other hand, the obtained k_{SQ} values are rather large for *cis*-*p*-2+, *trans*-*p*-2+, and ZnA-4+.

We compared the decrease ratios of excited lifetimes due to the self-quenching with those of the steady-state fluorescence intensities. The steady-state fluorescence intensities at 0.05% (I_0) and 70% (I_1) CEC conditions are expressed as eqs 4 and 5

$$I_0 = \frac{k_f}{k_d + k_f} \quad (4)$$

$$I_1 = \frac{k_f}{k_d + k_f + k_{SQ}} \quad (5)$$

According to eqs 4 and 5, the decrease ratio of steady-state fluorescence intensities can be expressed as eq 6

dx.doi.org/10.1021/jp309502j | J. Phys. Chem. A 2012, 116, 12065−12072

$$\frac{I_0}{I_1} = 1 + \frac{k_{SQ}}{k_d + k_f} \quad (6)$$

According to eqs 1 and 2, the decrease ratio of lifetimes can be expressed as eq 7

$$\frac{\tau_0}{\tau_1} = 1 + \frac{k_{SQ}}{k_d + k_f} \quad (7)$$

τ_0/τ_1 is plotted vs I_0/I_1 in Figure 4. The decrease ratios of lifetimes (τ_0/τ_1) due to the self-quenchings were almost the same as those of the steady-state fluorescence intensities (I_0/I_1). Thus, it was revealed again that the self-quenching in this clay/dye system was induced by the dynamic process.

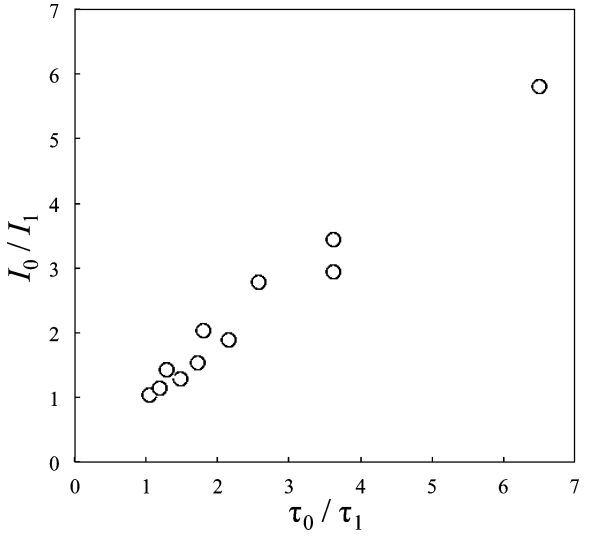

Figure 4. Relationship between the decrease ratios of lifetimes (τ_0/τ_1) and those of steady-state fluorescence intensities (I_0/I_1) due to the self-quenching. τ_0 and τ_1 are the excited lifetimes at 0.05% and 70% CEC conditions, respectively. I_0 and I_1 are the steady-state fluorescence intensities at 0.05% and 70% CEC conditions, respectively.

Relationship between the Self-Quenching Rate Constants and the Relative Adsorption Equilibrium Constant. What determines the self-quenching rate constants in clay/porphyrin complexes? As described in the Introduction, an electron transfer reaction and/or an enhanced thermal deactivation process due to the collision of molecules are probably the origin of self-quenching in this system. If the adsorbed porphyrins are completely fixed on the clay surface, the minimum center-to-center (edge-to-edge) distance between porphyrins is 2.87 nm (1.61 nm) under the 70% CEC condition. The average center-to-center distance between porphyrin molecules on the clay surface under the 70% CEC condition can be obtained by eq 8

$$R = \sqrt{\frac{2}{\sqrt{3}} \times \left(4 \times \frac{100}{70} \times 1.25\right)} \quad (8)$$

where R is the center-to-center distance between adjacent molecules on the basis of a hexagonal array, $(4 \times (100/70) \times 1.25)$ indicates the average area per one molecule (in nm^2), and 1.25 indicates the average area per one anionic charge of the examined clay (in nm^2).[13] Because the diameter of porphyrin molecule is 1.26 nm by the PM6 calculation,[43] the edge-to-edge distance under 70% CEC condition is determined to be 1.61 nm.

Since the distance is rather large to provoke the collision of molecules, it is assumed that porphyrin molecules are not completely fixed and can move on the clay surface.

Thus, we focused on the adsorption strength of porphyrin molecule on the clay surface. The adsorption strength, which is the quantitative barometer of the host (clay)−guest (molecule) interaction, should affect the mobility of porphyrin molecules on the clay surface. The high mobility of porphyrin molecules on the clay surface should enhance the probability of efficient collision.

Following the experimental procedure in the Experimental Section, the relative adsorption equilibrium constants K_{rel} of porphyrin molecules on the clay surface were determined for discussing the adsorption strength according to eq 9[7]

$$P/\text{clay} + A \rightleftarrows A/\text{clay} + P \quad (9)$$

where P/clay and A/clay are the adsorbed amount of *p*-4+ and the additional porphyrin on the clay surface, respectively, and P and A are the amount of *p*-4+ and the additional porphyrin in a bulk solution, respectively. The observed absorption spectra corresponded well to the sum of individual absorption spectra of *p*-4+ and the additional porphyrin in the bulk solution and on the clay surface.

From eq 8, relative adsorption equilibrium constant K_{rel} is expressed as eq 10[7]

$$K_{rel} = \frac{[P][A/\text{clay}]}{[P/\text{clay}][A]} \quad (10)$$

The obtained values of K_{rel} are summarized in Table 3. *p*-4+ was used as a standard of K_{rel}. The differences of K_{rel} can be explained by porphyrin structures such as the presence of center metal and number of cationic sites and *meso*-substituents, as reported in the previous paper.[7]

Table 3. Relative Adsorption Equilibrium Constant K_{rel}[a]

	K_{rel}
p-4+	1
m-4+	0.12[b]
o-4+	0.0016[b]
A-4+	0.42
p-3+	0.81
m-3+	0.1
o-3+	0.0013
cis-*p*-2+	0.35[b]
trans-*p*-2+	0.43[b]
Zn*p*-4+	0.3[b]
Zn*A*-4+	0.27

[a] *p*-4+ was used as a standard of K_{rel}. [b] Values refer to ref 7.

The obtained K_{rel} values are plotted vs k_{SQ} in Figure 5. As shown in Figure 5, a correlation between K_{rel} and k_{SQ} was not observed. Why was a correlation not observed?

The major factors governing the adsorption equilibrium constant of porphyrin molecules on the clay surface would be hydrophobic and coulombic interactions. Of these, the hydrophobic interaction would not affect the collision frequency of porphyrin molecules on the clay surface, because the strength of hydrophobic interaction is not governed by anionic sites of clay surface. In other words, the strength of hydrophobic interaction, which is typically determined by the

dx.doi.org/10.1021/jp309502j | J. Phys. Chem. A 2012, 116, 12065−12072

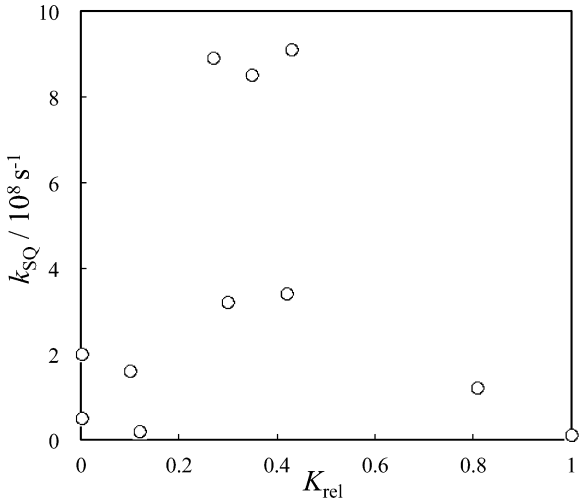

Figure 5. Relationship between K_{rel} and k_{SQ}.

molecular area, is almost constant when porphyrin exists anywhere on the clay surface.

On the other hand, since the coulombic interaction is governed by the distance between the cationic sites of porphyrin and the anionic site of clay surface, it is governed by the location of molecule and should affect the mobility and the collision frequency of guests. Thus, it is assumed that K_{rel}, which includes both hydrophobic and coulombic interactions, does not correlate with k_{SQ}. We again attempted to have a relationship between k_{SQ} and the coulombic interactions in the next section.

Relationship between the Self-Quenching Rate Constants and the Coulombic Interaction between Porphyrin and Clay. The relationship between k_{SQ} and the coulombic interaction is discussed. The coulombic attraction energy V (in kcal mol^{-1}) is expressed as eq 11

$$V = q_1 q_2 N_A / 4\pi\varepsilon\varepsilon_0 r \quad (11)$$

where q_1 and q_2 are the electrical charge of matter$_1$ and matter$_2$, respectively, N_A is the Avogadro constant, ε is the relative permittivity of water (79.87 in 293 K), ε_0 is the dielectric constant under vacuum (8.85×10^{-12} C^2 J^{-1} m^{-1}), and r is the distance between matter$_1$ and matter$_2$ (in m).

The V values between porphyrin and clay are calculated as follows. In this calculation, the charges in porphyrin molecules and clay surface are defined to be localized in the center of N atom in *meso*-substituent and the center of O atoms surrounding Al atom,[44] respectively. The intercationic site distances in porphyrin molecules were calculated by the PM6, as summarized in Table 4.[8,13,14] In the present system, the average interanionic site distance on the clay surface is 1.2 nm on the basis of a hexagonal array.

To determine the r values, the dihedral angles between porphyrin ring and *meso*-substituents are necessary because the z-coordinate component of r values highly depends on the dihedral angle. The dihedral angles were determined by calculating the optimized structure of clay/porphyrin complexes as described below. Each optimized structure of porphyrin molecule and clay sheet was calculated by the PM6, respectively. In this calculation, the surficial tetrahedral sheet including four anionic sites was used as the clay sheet. They were combined, and the optimized structure of clay/porphyrin complex was calculated with fixing the clay structure and the porphyrin structure without dihedral angles. The typical calculated structure for *p*-4+/clay complex is shown in Figure 6. The calculations were successfully conducted for *p*-4+, *m*-4+, *o*-4+, and *A*-4+, and the obtained dihedral angles are shown in Table 4. The obtained values of dihedral angles from the vertical are reasonable for the aspect of the steric hindrance of *meso*-substituents; that is, the dihedral angles are large for *o*-4+ and *A*-4+, which have large steric hindrances. The dihedral angles for other porphyrins were diverted from *p*-4+, *m*-4+, *o*-4+, and *A*-4+, which have the same *meso*-substituent.

From the intercationic distances in porphyrin molecule and the dihedral angles, the distances between cationic sites of porphyrin and the nearest anionic site of clay were determined to be r_1, r_2, r_3, and r_4. The sum of coulombic attraction energy (V_{sum}) was calculated by the total of V_1, V_2, V_3, and V_4 that are determined by the corresponding distances (r_1, r_2, r_3, and r_4).

In the case of Zn porphyrins, the existence of water molecule as a weak axial ligand will decrease V values. By using a diameter of 0.3 nm for water molecule, the V_{sum} value can be recalculated for Zn*p*-4+ when water molecule exists as a weak

Table 4. Calculated Values of Intercationic Charge Distances in Porphyrin Molecules, Dihedral Angles between Porphyrin Ring and *meso*-Substituent from the Vertical, Distances between Cationic Sites of Porphyrin and the Nearest Anionic Site on the Clay (r_1, r_2, r_3, r_4), Corresponding Coulombic Attraction Energies (V_1, V_2, V_3, V_4), and Sum of Coulombic Attraction Energies (V_{sum})

	intercationic distance/nm	dihedral angle/deg	r_1/nm (V_1/kcal mol^{-1})	r_2/nm (V_2/kcal mol^{-1})	r_3/nm (V_3/kcal mol^{-1})	r_4/nm (V_4/kcal mol^{-1})	V_{sum}/kcal mol^{-1}
p-4+	1.05	42	0.36 (1.15)	0.44 (0.94)	0.36 (1.15)	0.44 (0.94)	4.18
m-4+	0.99	45	0.43 (0.97)	0.54 (0.77)	0.43 (0.97)	0.54 (0.77)	3.48
o-4+	0.88	60	0.47 (0.88)	0.63 (0.66)	0.47 (0.88)	0.63 (0.66)	3.08
A-4+	1.33	63	0.56 (0.74)	0.64 (0.65)	0.56 (0.74)	0.64 (0.65)	2.78
p-3+	1.05	42[a]	0.36 (1.15)	0.44 (0.94)	0.36 (1.15)	–	3.24
m-3+	0.99	45[b]	0.43 (0.97)	0.54 (0.77)	0.43 (0.97)	–	2.71
o-3+	0.88	60[c]	0.47 (0.88)	0.63 (0.66)	0.47 (0.88)	–	2.42
cis-*p*-2+	1.05	42[a]	0.33 (1.25)	0.33 (1.25)	–	–	2.50
trans-*p*-2+	1.41	42[a]	0.34 (1.22)	–	0.34 (1.22)	–	2.44
Zn*p*-4+	1.05	42[a]	0.36 (1.15)	0.44 (0.94)	0.36 (1.15)	0.44 (0.94)	4.15
			0.93 (0.45)[e]	0.97 (0.43)[e]	0.93 (0.45)[e]	0.97 (0.43)[e]	2.81[e]
Zn*A*-4+	1.33	63[d]	0.56 (0.74)	0.64 (0.65)	0.56 (0.74)	0.64 (0.65)	2.78

[a]Values are diverted from *p*-4+. [b]Values are diverted from *m*-4+. [c]Values are diverted from *o*-4+. [d]The value is diverted from *A*-4+. [e]Recalculated value considering the coordination of water molecule on porphyrin center metal (Zn).

dx.doi.org/10.1021/jp309502j | J. Phys. Chem. A 2012, 116, 12065−12072

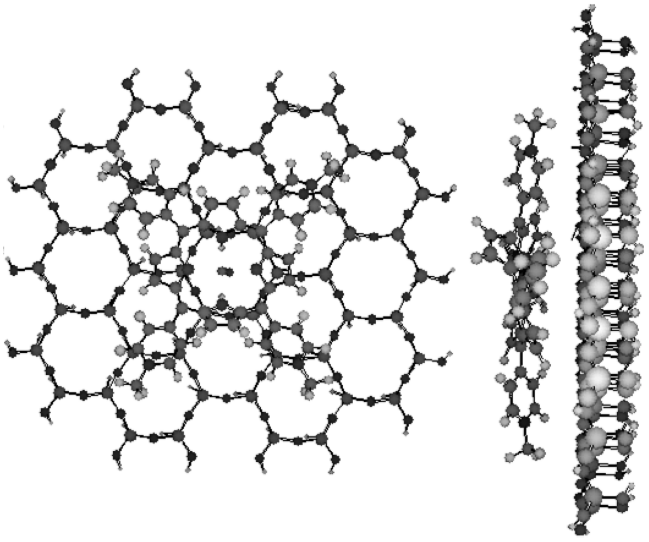

Figure 6. Optimized structure of *p*-4+ on the clay surface by the PM6 calculation (left, top view; right, side view). The surficial tetrahedral layer of the clay was only applied for the calculation.

axial ligand. Because the steric hindrance of trimethylanilinium group in Zn*A*-4+ is larger than that of water molecule, a recalculation was not conducted for Zn*A*-4+. These calculation procedures are summarized in Table 4.

The sums of calculated coulombic attraction energies (V_{sum}) are plotted vs k_{SQ} in Figure 7. As shown in Figure 7, a good correlation was observed.

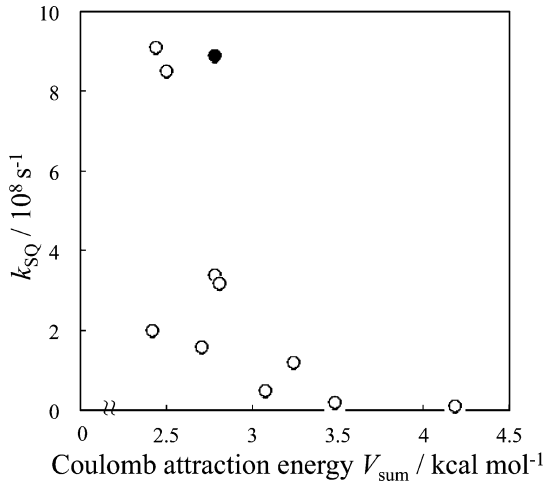

Figure 7. Relationship between the sum of coulombic attraction energy (V_{sum}) and k_{SQ}. ● indicates Zn*p*-4+ and Zn*A*-4+.

Among the examined porphyrins, *p*-4+ has the strongest coulombic interaction , and the self-quenching was almost negligible. On the other hand, large self-quenchings were observed for porphyrins which have relatively weak coulombic interactions.

It was found that the self-quenching behavior of adsorbed porphyrins depends on the coulombic interaction. That is, a strong coulombic interaction suppresses mobility and collision frequency of guests on the clay surface, indicating that the collision of guest molecules was revealed as the origin of unfavorable quenching on solid surfaces. This novel finding of self-quenching process on the solid surfaces will play an important role in developing efficient photochemical reaction systems.

CONCLUSION

The self-quenching behavior of cationic porphyrin molecules adsorbed on an anionic clay surface was systematically investigated by using the 11 types of porphyrin molecules differing in their center metal, *meso*-substituent, and the number of cationic sites. Because the aggregation of porphyrin molecules on the clay surface is completely suppressed by the previously reported "size-matching rule", the self-quenching is probably induced by an electron transfer and/or an enhanced thermal deactivation process due to the collision of porphyrin molecules on the clay surface. By measuring the steady-state and time-resolved fluorescence spectra of clay/porphyrin complexes, the self-quenching rate constants were determined to be 0.1−9.1 × 10^8 s^{-1}. By the systematic experiments, it was found that the quenching rate constants correlated well with the strengths of coulombic interaction between host and guest. The strong coulombic interaction should suppress the mobility and collision frequency of guests on the clay surface; thus, the collision of guest molecules was revealed as the origin of unfavorable quenching for photochemical reactions on the clay surface. According to this principle, we will be able to construct efficient photochemical reaction systems without any quenching process, such as efficient energy transfers toward an artificial light-harvesting system.

ASSOCIATED CONTENT

Supporting Information

Time-resolved fluorescence spectra. This material is available free of charge via the Internet at http://pubs.acs.org.

AUTHOR INFORMATION

Corresponding Author

*E-mail takagi-shinsuke@tmu.ac.jp; tel. +81 42 677 2839; fax +81 42 677 2838.

Notes

The authors declare no competing financial interest.

ACKNOWLEDGMENTS

This work has been partly supported by a Grant-in-Aid for Precursory Research for Embryonic Science and Technology (PRESTO) from the Japan Science and Technology Agency (JST) and JSPS Research Fellow DC1 from the Japan Society for the Promotion of Science.

REFERENCES

(1) Casey, J. P.; Bachilo, S. M.; Weisman, R. B. *J. Mater. Chem.* **2008**, *18*, 1510−1516.
(2) Kaschak, D. M.; Lean, J. T.; Waraksa, C. C.; Saupe, G. B.; Usami, H.; Mallouk, T. E. *J. Am. Chem. Soc.* **1999**, *121*, 3435−3445.
(3) Sen, T.; Hana, S.; Koner, S.; Patra, A. *J. Phys. Chem. C* **2010**, *114*, 19667−19672.
(4) Sun, X.; Zhao, Y.; Lin, V. S. Y.; Slowing, I. I.; Trewyn, B. G. *J. Am. Chem. Soc.* **2011**, *133*, 18554−18557.
(5) Yui, T.; Kobayashi, Y.; Yamada, Y.; Yano, K.; Fukushima, Y.; Torimoto, T.; Takagi, K. *ACS Appl. Mater. Interfaces* **2011**, *3*, 931−935.
(6) Inagaki, S.; Ohtani, O.; Goto, Y.; Okamoto, K.; Ikai, M.; Yamanaka, K.; Tani, T.; Okada, T. *Angew. Chem. Ind. Ed.* **2009**, *48*, 4042−4046.

(7) Ishida, Y.; Masui, D.; Shimada, T.; Tachibana, H.; Inoue, H.; Takagi, S. *J. Phys. Chem. C* **2012**, *116*, 7879−7885.
(8) Takagi, S.; Tryk, D. A.; Inoue, H. *J. Phys. Chem. B* **2002**, *106*, 5455−5460.
(9) Takagi, S.; Eguchi, M.; Tryk, D. A.; Inoue, H. *Langmuir* **2006**, *22*, 1406−1408.
(10) Takagi, S.; Eguchi, M.; Inoue, H. *Res. Chem. Intermed.* **2007**, *33*, 177−189.
(11) Ishida, Y.; Shimada, T.; Masui, D.; Tachibana, H.; Inoue, H.; Takagi, S. *J. Am. Chem. Soc.* **2011**, *13*, 14280−14286.
(12) Takagi, S.; Shimada, T.; Yui, T.; Inoue, H. *Chem. Lett.* **2001**, *30*, 128−129.
(13) Takagi, S.; Shimada, T.; Eguchi, M.; Yui, T.; Yoshida, H.; Tryk, D. A.; Inoue, H. *Langmuir* **2002**, *18*, 2265−2272.
(14) Eguchi, M.; Takagi, S.; Tachibana, H.; Inoue, H. *J. Phys. Chem. Solids* **2004**, *65*, 403−407.
(15) Egawa, T.; Watanabe, H.; Fujimura, T.; Ishida, Y.; Yamato, M.; Masui, D.; Shimada, T.; Tachibana, H.; Inoue, H.; Takagi, S. *Langmuir* **2011**, *27*, 10722−10729.
(16) Takagi, S.; Eguchi, M.; Inoue, H. *Res. Chem. Intermed.* **2007**, *33*, 177−189.
(17) Fujii, K.; Iyi, N.; Hashizume, H.; Shimomura, S.; Ando, T. *Chem. Mater.* **2009**, *21*, 1179−1181.
(18) Kuroda, T.; Fujii, K.; Sakoda, K. *J. Phys. Chem. C* **2010**, *114*, 983−989.
(19) Schanze, K.; Silverman, E. E.; Zhao, X. *J. Phys. Chem. B* **2005**, *109*, 18451−18459.
(20) Ahmad, A.; Kurkina, T.; Kern, K.; Balasubramanian, K. *Chem. Phys. Chem* **2009**, *10*, 2251−2255.
(21) Phillips, R. L.; Kim, I. B.; Tolbert, L. M.; Bunz, U. H. F. *J. Am. Chem. Soc.* **2008**, *130*, 6952−6954.
(22) Sohmiya, M.; Ogawa, M. *Microporous Mesoporous Mater.* **2011**, *142*, 363−370.
(23) Zhang, B.; Zhang, Y.; Mallapragada, S. K.; Clapp, A. R. *ACS Nano* **2011**, *5*, 129−138.
(24) Evans, T. R. *J. Am. Chem. Soc.* **1971**, *93*, 2081−2082.
(25) Boulu, L. G.; Patterson, L. K.; Chauvet, J. P.; Kozak, J. J. *J. Chem. Phys.* **1987**, *86*, 503−507.
(26) Ogi, T.; Benten, H.; Ito, S. *Thin Solid Films* **2007**, *515*, 3107−3111.
(27) Perrin, F. *Hedb. Seances Acad. Sci.* **1924**, *178*, 1978−1980.
(28) Nakaema, M. K. K.; Leite, B. B. P.; Sanches, R. *Arch. Biochem. Biophys.* **1997**, *1*, 61−66.
(29) Nagai, K.; Nishijima, T.; Takamiya, N.; Tada, M.; Kaneko, M. *J. Photochem. Photobiol., A* **1995**, *92*, 47−51.
(30) Brown, R. S.; Brennan, J. D.; Krull, U. J. *J. Chem. Phys.* **1994**, *100*, 6019−6027.
(31) Chattopadhyay, A.; London, E. *Biochem.* **1987**, *26*, 39−45.
(32) Okada, T.; Ide, Y.; Ogawa, M. *Chem. − Asian J.* **2012**, *7*, 1980−1992.
(33) Lopez Arbeloa, F.; Martinez Martiınez, V.; Arbeloa, T.; Lopez Arbeloa, I. *J. Photochem. Photobiol., C* **2007**, *8*, 85−108.
(34) Ras, R.; Umemura, Y.; Johnston, C.; Yamagishi, A.; Schoonheydt, R. *Phys. Chem. Chem. Phys.* **2007**, *9*, 918−932.
(35) Sato, H.; Hiroe, Y.; Tamura, K.; Yamagishi, A. *J. Phys. Chem. B* **2005**, *109*, 18935−18941.
(36) Letaief, S.; Detellier, C. *Langmuir* **2009**, *25*, 10975−10979.
(37) Takagi, K.; Shichi, T. *J. Photochem. Photobiol., C* **2000**, *1*, 113−130.
(38) Thomas, J. K. *Chem. Rev.* **1993**, *93*, 301−320.
(39) Bujdak, J.; Komadel, P. *J. Phys. Chem. B* **1997**, *101*, 9065−9068.
(40) Bujdak, J.; Iyi, N.; Fujita, T. *Clay Miner.* **2002**, *37*, 121−133.
(41) Viaene, K.; Caigui, J.; Schoonheydt, R. A.; De Schryver, F C. *Langmuir* **1987**, *3*, 107−111.
(42) Pushpito, G. K.; Bard, A. *J. Phys. Chem.* **1984**, *88*, 5519−5526.
(43) Stewart, J. J. P. *J. Mol. Graphics Modell.* **2004**, *10*, 6−12.
(44) Bleam, W. F.; Hoffmann, R. *Inorg. Chem.* **1988**, *27*, 3180−3186.